JACC Vol. 27, No. 2
February 1996:399–406

Mechanisms of Hemolysis With Mitral Prosthetic Regurgitation

Study Using Transesophageal Echocardiography and Fluid Dynamic Simulation

MARIO J. GARCIA, MD, PIETER VANDERVOORT, MD, WILLIAM J. STEWART, MD, FACC, BRUCE W. LYTLE, MD, FACC, DELOS M. COSGROVE III, MD, FACC, JAMES D. THOMAS, MD, FACC, BRIAN P. GRIFFIN, MD, FACC

Cleveland, Ohio

Objectives. **The aims of this study were to define the hydrodynamic mechanisms involved in the occurrence of hemolysis in prosthetic mitral valve regurgitation and to reproduce them in a numeric simulation model in order to estimate peak shear stress.**

Background. **Although in vitro studies have demonstrated that shear stresses >3,000 dynes/cm^2 are associated with significant erythrocyte destruction, it is not known whether these values can occur in vivo in conditions of abnormal prosthetic regurgitant flow.**

Methods. **We studied 27 patients undergoing reoperation for significant mitral prosthetic regurgitation, 16 with and 11 without hemolysis. We classified the origin and geometry of the regurgitant jets by using transesophageal echocardiography. By using the physical and morphologic characteristics defined, several hydrodynamic patterns were simulated numerically to determine shear rates.**

Results. **Eight (50%) of the 16 patients with hemolysis had paravalvular leaks and the other 8 had a jet with central origin, in contrast to 2 (18%) and 9 (82%), respectively, of the 11 patients without hemolysis ($p = 0.12$, power 0.38). Patients with hemolysis had patterns of flow fragmentation (n = 2), collision (n = 11) or rapid acceleration (n = 3), whereas those without hemolysis had either free jets (n = 7) or slow deceleration (n = 4) ($p < 0.001$, power 0.99). Numeric simulation demonstrated peak shear rates of 6,000, 4,500, 4,500, 925 and 450 dynes/cm^2 in these five models, respectively.**

Conclusions. **The distinct patterns of regurgitant flow seen in these patients with mitral prosthetic hemolysis were associated with rapid acceleration and deceleration or high peak shear rates, or both. The nature of the flow disturbance produced by the prosthetic regurgitant lesion and the resultant increase in shear stress are more important than the site of origin of the flow disturbance in producing clinical hemolysis.**

(J Am Coll Cardiol 1996;27:399–406)

Since the implantation of the first mechanical prosthesis by Hufnagel in 1956, traumatic hemolysis has been recognized as a potentially serious complication following valve replacement (1–3). This complication is rarely seen now with normally functioning prostheses but is still encountered in the setting of prosthetic dysfunction, especially with periprosthetic regurgitation (4–17). High shear stress forces with abnormal flow jets seen in prosthetic dysfunction are thought to be an important cause of hemolysis (18–20). In vitro studies have demonstrated that shear stress forces >3,000 dynes/cm^2 are associated with significant erythrocyte destruction (21). However, whether these shear values can occur clinically in conditions of abnormal prosthetic regurgitant flow has not yet been studied.

Transesophageal echocardiography is increasingly used in the evaluation of prosthetic dysfunction and is particularly useful in the assessment of the site and mechanism of prosthetic regurgitation (22–24). Biplane and multiplane imaging probes with two-dimensional echocardiographic and color Doppler mapping capabilities can be used to define the location and size of abnormal regurgitant flow jets with respect to the surrounding prosthesis and other tissue interfaces. By using information about location of jets, pressure gradients and basic fluid dynamics, flow patterns can be simulated to detail the spatial velocity distribution around the prostheses and to estimate the shear stress occurring at peak flow. Therefore, the aims of this study were 1) to define the hydrodynamic mechanisms involved in the occurrence of hemolysis in prosthetic mitral regurgitation by transesophageal echocardiography, and 2) to reproduce these mechanisms by using computer numeric simulation to estimate peak shear stress and any other unusual physical flow features for each of these mechanisms.

Methods

Patient selection. The study group consisted of 27 consecutive patients undergoing reoperation for significant mitral

From the Cardiovascular Imaging Center, Departments of Cardiology and Cardiothoracic Surgery, The Cleveland Clinic Foundation, Cleveland, Ohio. This study was supported in part by Grant-in-Aid 93-013380 from the American Heart Association, Dallas, Texas (Dr. Thomas). It was presented in part at the 43rd Annual Scientific Session of the American College of Cardiology, Atlanta, Georgia, March 1994.

Manuscript received July 20, 1994; revised manuscript received April 25, 1995, accepted May 5, 1995.

Address for correspondence: Dr. Brian P. Griffin, Desk F-15, Division of Cardiology, The Cleveland Clinic Foundation, 9500 Euclid Avenue, Cleveland, Ohio 44195.

Published by Elsevier Science Inc.

0735-1097/96/$15.00
0735-1097(95)00403-Q

JACC Vol. 27, No. 2
February 1996:399–406

Table 1. Clinical Characteristics of the 27 Study Patients

	Patients With Hemolysis (n = 16)	Patients Without Hemolysis (n = 11)	p Value
Age (yr)	62 ± 10.3	69 ± 7.5	0.07
Men	9	6	1.00
Indications for operation			
Congestive heart failure	13	10	0.62
Hemolysis	7	0	0.02
Hematocrit (%)	27.7 ± 3.6%	39.9 ± 5.3%	< 0.001
Total bilirubin	3.6 ± 2.7	1.6 ± 0.5	0.03
Lactic dehydrogenase (IU)			
Preoperative	2,443 ± 1,672	256 ± 37	< 0.001
Postoperative	497 ± 135*	238 ± 35†	< 0.001

*p < 0.001 versus preoperative lactic dehydrogenase in the hemolysis group. †p = NS versus preoperative lactic dehydrogenase in the group without hemolysis. Values are expressed as mean value ± SD or number of patients.

prosthetic regurgitation. Patients with confounding variables such as multiple prostheses or native valvular disease likely to predispose to hemolysis were excluded. The patients were assigned to two groups on the basis of their serum hematocrit and lactic dehydrogenase levels: 1) hemolysis group (hematocrit <33%, lactic dehydrogenase ≥800 IU, n = 16), and 2) control group (patients without hemolysis: hematocrit ≥33%, lactic dehydrogenase <800 IU, n = 11). The clinical characteristics of each group are given in Table 1.

Hemolysis group. These 16 patients had evidence of significant traumatic red blood cell destruction (hematocrit 27.7% [range 21% to 33%], lactic dehydrogenase 2,443 IU [range 826 to 6,354]) as a result of their prosthetic dysfunction. The diagnosis of valve-induced hemolysis was further supported by the presence of typical changes in the peripheral blood smear (fragmentation, poikilocytosis, and spherocytosis) and by a reduction before hospital discharge ≥50% of the baseline level of lactic dehydrogenase. We excluded patients with a past or family history of hemolytic anemia or a cause other than prosthetic dysfunction that might have contributed to the hemolytic anemia. Six of the 16 patients in the hemolysis group had significant jaundice and hemoglobinuria, and eight required multiple blood transfusions before their corrective surgery. Seven of the 16 had a mechanical prosthesis, 6 had a bioprosthetic valve and 3 had prior repair with insertion of a prosthetic annular ring. The interval between the initial and the second surgical intervention was 75 months (range 1 to 197) in the hemolysis group.

Control group (patients without hemolysis). Patients in this group had severe mitral prosthetic regurgitation without evidence of significant hemolytic anemia (hematocrit 39.9% [range 33% to 48%], lactic dehydrogenase 255 IU [range 177 to 301]). Four patients had a mechanical prosthesis, five a bioprosthesis and one a prior repair (Table 2). The interval between the initial and the second surgical intervention was 93 months (range 1 to 219) in the control group (p = NS, compared with the interval in the hemolysis group).

Table 2. Malfunctioning Prosthetic Valve Type

	Patients With Hemolysis	Patients Without Hemolysis
Mechanical	7	4
Bioprosthesis	6	5
Previous repair	3	2
	(p = 0.55, power 0.06)	

Transesophageal echocardiography. All patients were studied with transesophageal echocardiography before reoperation. The studies were performed with a Hewlett-Packard Sonos 1000 or 1500 or an Acuson 128 XP/10 attached to a biplane or multiplane transesophageal transducer. The mitral valve prostheses were evaluated to determine the site, severity and hydrodynamic characteristics of the regurgitant jet. The studies were recorded on 0.5-in. (1.27-cm) videotape for subsequent retrieval and analysis. The studies were analyzed off-line by two experienced echocardiographers.

Site of mitral regurgitation. Regurgitation was defined as central or paravalvular depending on its site of origin within the sewing ring (central) or outside of the sewing ring (paravalvular). The number of regurgitant sites was also documented. The Doppler echocardiographic findings were independently validated by the surgical findings at operation.

Severity of mitral regurgitation. Mitral regurgitation was classified semiquantitatively on the basis of previously published methods (25,26) using the depth of penetration of the regurgitant jet within the left atrial cavity and the characteristics of the pulmonary venous pulsed Doppler tracing.

Hydrodynamic characteristics of the regurgitant jet. The mitral regurgitant jet was interrogated by color flow mapping in multiple views. The geometry of the jet was classified into five patterns (Fig. 1). 1) *Fragmentation:* Characterized by a regurgitant jet that is divided by a solid structure such as a free floating suture, a redundant chord or a dehisced annuloplasty ring. 2) *Collision:* Sudden deceleration of the regurgitant jet by a solid structure situated close to the origin of the jet and perpendicular to the jet direction. This was most often the limbus of the left atrial appendage. 3) *Acceleration:* Characterized by the presence of a regurgitant jet through a small orifice (<2 mm in diameter) such as a leaflet perforation or a small single or multiple paravalvular leaks, with no direct impact on any solid structure. 4) *Free jet:* A regurgitant jet with a larger diameter at origin (>2 mm) that is not constrained by solid structures until it reaches the posterosuperior wall of the left atrium. 5) *Slow deceleration:* A jet originating from a large eccentric orifice that is deflected in a curved trajectory along the atrial wall from its point of origin.

Numeric flow simulation. The hydrodynamic patterns just described were simulated in a two-dimensional or axisymmetric finite difference grid with an 80486-based microcomputer using commercially available software (Fluent version 4.11). The numeric models developed were idealized geometric configurations based on the real-life physical and morphologic

characteristics defined in patients with transesophageal echocardiography. A variable flow input was used to obtain a maximal velocity (v) at the regurgitant orifice of 5 m/s, because in most clinical conditions the peak mitral regurgitation jet velocity will approximate this value ($4v^2 \cong 100$ mm Hg = difference between simultaneous systolic left ventricular and left atrial pressures).

The computer models were constructed as follows (Fig. 1): 1) *Fragmentation:* Free laminar flow with a peak velocity of 5 m/s was simulated with a horizontal vector in a rectangular grid formed by 44 × 82 square cells of 100 μm on each side. The flow was divided by a 0.3-mm diameter solid structure located in the center of the jet.

2) *Collision:* In a rectangular grid with the dimensions of the preceding model, two parallel horizontal walls were simulated at a distance of 0.3 mm from the horizontal midline and extending through a distance of 1 mm. A vertical wall was simulated at 1.5 mm distal to the end of the horizontal walls. A laminar flow jet with a peak velocity of 5 m/s with a horizontal vector was simulated as passing between the two horizontal walls and colliding with the vertical wall.

3) *Rapid acceleration:* An axisymmetric grid of 64 × 62 square cells with dimensions of 100 μm on each side was used in this model. A vertical wall with a central orifice 1-mm in diameter was located close to the vertical midline.

4) *Free jet:* This model was similar to model 3 but had an orifice diameter of 4 mm. The proximal flow velocity was increased to achieve a peak velocity of 5 m/s at the orifice.

5) *Slow deceleration:* A rectangular grid of 54 × 60 square cells with a diameter of 100 μm each was used in this model. Two oblique walls converging to a central orifice and another two oblique diverging walls were constructed near the center of the grid with a slight misalignment to obtain an oblique orifice 4.1 mm in diameter. Flow with a horizontal vector was simulated proximal to the wall to achieve a maximal velocity of ~5 m/s distal to the wall.

Determination of shear stress. Our computer simulation used the Navier-Stokes equations for incompressible flow: $\nabla \cdot \mathbf{v} = 0$, where ∇ is the differential operator on velocity $\mathbf{v}$, a three-component velocity vector, and $\rho(Dv/Dt) = -\nabla p + \mu\nabla^2\mathbf{v}$, where Dv/Dt is the "material" derivative for moving fluid, a vector operator for which the x-component of velocity (in cartesian coordinates) is

$$i\left(\frac{\partial v_x}{\partial t} + v_x\frac{\partial v_x}{\partial x} + v_y\frac{\partial v_x}{\partial y} + v_z\frac{\partial v_x}{\partial z}\right);$$

$\mathbf{v}$ is the local three-dimensional velocity vector; ρ is local pressure; and μ is viscosity. A finite number of iterations (range 500 to 3,000) was required before the model converged to a stable velocity map for each model. Shear stress value was calculated by the formula: $S = \mu(\partial v/\partial r)$, where S = shear; μ = viscosity of blood (0.03 g/cm × s^{-1}); v = velocity at each cell; and r = size of the cell. The shear at each coordinate was calculated in the x and the y directions, the maximal value obtained, and its location was noted for each model (Fig. 1).

For display purposes, the simulations were repeated with a coarser discretization mesh, allowing a more complete view of the left atrium, left ventricle and mitral valve to be shown. However, all shear calculations were obtained from the 100-μ grid simulations.

Spatial and temporal acceleration. We also explored the effect of orifice size on the instantaneous acceleration experienced by an erythrocyte. For this we modeled axisymmetric flow passing at 5 m/s through round orifices with diameters of 8, 0.8 and 0.08 mm. Spatial acceleration was calculated as $\partial v_x/\partial x$, whereas peak temporal acceleration (which would be experienced by an individual erythrocyte within the flow) was given by $v_x(\partial v_x/\partial x)$.

Statistical analysis. We used the chi-square test (or Fisher exact test, where appropriate) to test for a difference in prevalence between the hemolysis and control groups with regard to 1) type of prosthesis (mechanical, biologic or annular ring); 2) site of regurgitation (valvular or paravalvular) and 3) jet morphology (patterns 1 through 5, as defined earlier). Unpaired t tests were used to compare continuous variables. Significance was assumed at a p level < 0.05.

Results

Patients with hemolysis had significantly higher levels of lactic dehydrogenase and bilirubin and lower hematocrit values than those of the control patients without hemolysis, but age and gender in the two groups were similar (Table 1). The two groups had mechanical, biologic and annular devices in similar proportions (Table 2).

Site of mitral regurgitation. The regurgitant jet was central in origin in eight patients in the hemolysis group (50%) and nine patients in the control group (81%) (p = 0.12, power 0.38, 95% confidence interval [CI] of difference −0.68 to 0.06). The other patients had paravalvular leaks (Table 3). No patient in either group had both a paravalvular and a central jet. Paravalvular jets had multiple sites of origin in three patients with and in one patient without hemolysis. Central jets were seen in eight patients with a bioprosthetic valve, five with a mechanical prosthesis and three with a repair, with a leak between the ring and the patient's mitral annulus. Paravalvular leaks were seen in five patients with a bioprosthesis, four with mechanical prosthesis and two with a repair (p = 0.96, power 0.05).

Hydrodynamic mechanisms of regurgitation. Table 3 summarizes the classification according to the mechanisms in the patients with and without hemolysis. In the hemolysis group, all patients had either fragmentation (n = 2), rapid acceleration (n = 3) or collision (n = 11), in contrast to the control group patients, who had either a free jet (n = 7) or slow deceleration (n = 4) (p < 0.001, power 0.99). In the two patients with fragmentation, the regurgitant jet was divided by a loose suture in one and a dehiscent ring in the other. In 7 of the 11 patients with collision, a paravalvular leak through a large orifice was located near the lateral portion of the mitral ring; the regurgitant jet was directed toward the wall of the atrial appendage, located 3 to 8 mm from the regurgitant orifice. In the other four patients with collision a central jet

JACC Vol. 27, No. 2
February 1996:399–406

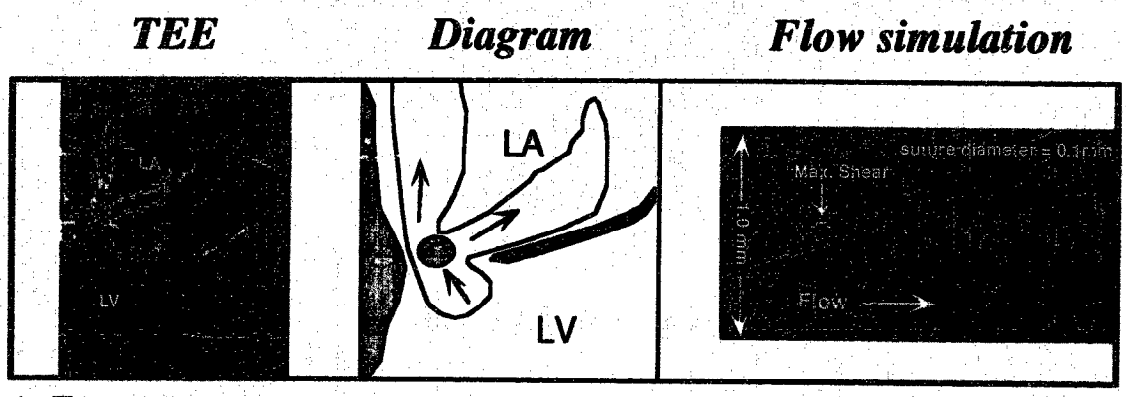

A. Fragmentation

A regurgitant jet is divided by a dehisced annular support ring.

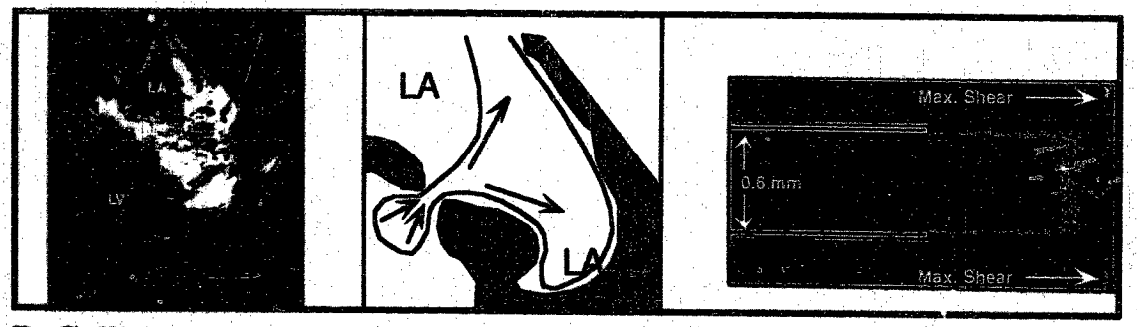

B. Collision

A paravalvular regurgitant jet is suddenly decelerated when colliding with the left atrial appendage wall.

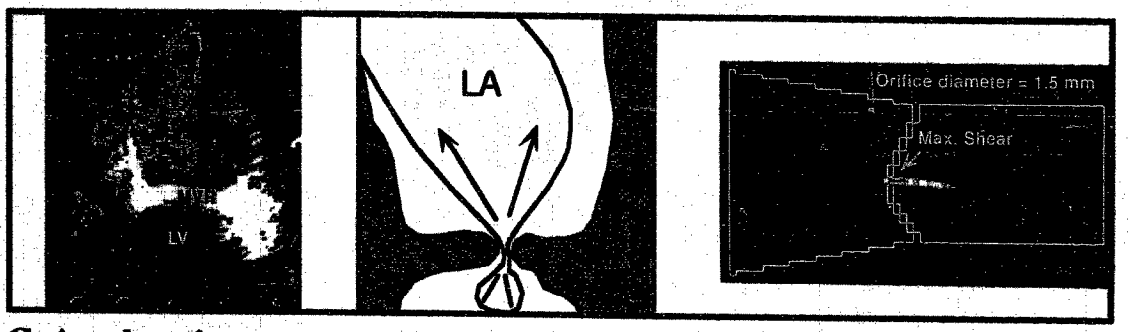

C. Acceleration

A jet is seen traversing through a small perforation in a thickened degenerated bioprosthesis.

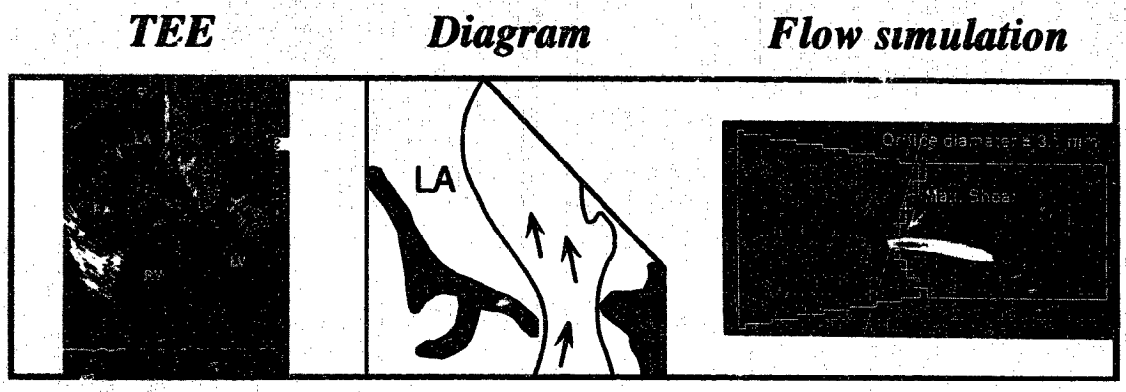

A. Free Jet

A central jet travels through a large orifice in a bioprosthesis with a torn cusp.

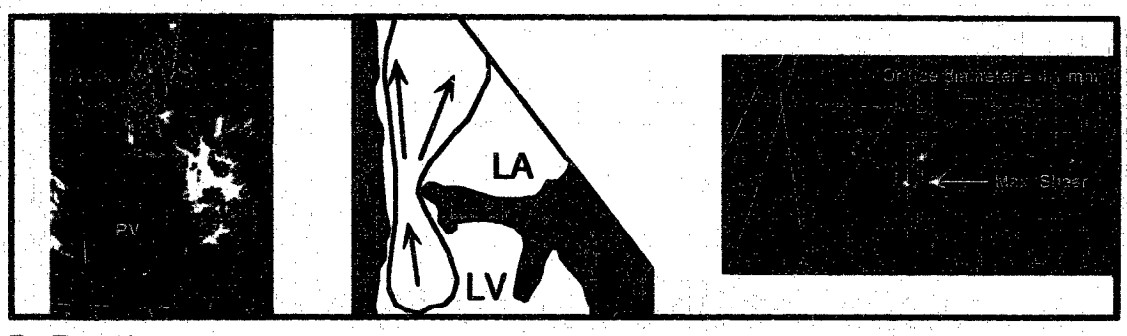

B. Deceleration

A large paravalvular mitral regurgitation jet slides gently along the atrial wall.

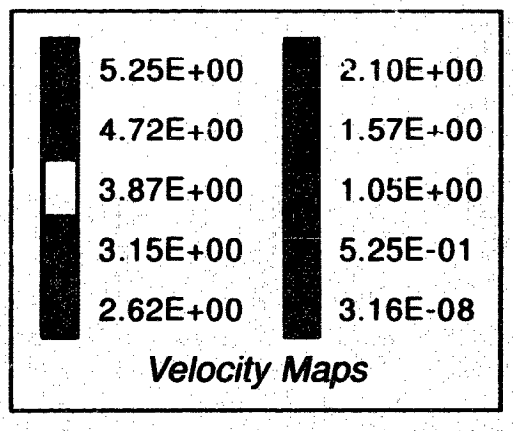

Figure 1. Patterns of regurgitant flow with (page 402) and without hemolysis (page 403). Shear stress is calculated at each location in the numeric grid using the velocity gradients and the known distances. The areas where peak shear rate occurs are shown in each model (**white arrows**). The models displayed here were done with a coarse discretization mesh to demonstrate the full extension of the jets. Velocity maps are color encoded, and values expressed in m/s. AO = aorta; LA = left atrium; LAA = left atrial appendage; LV = left ventricle; MVR = mitral prosthesis; R = prosthetic ring; RA = right atrium; RV = right ventricle; TEE = transesophageal echocardiography.

JACC Vol. 27, No. 2
February 1996:399–406

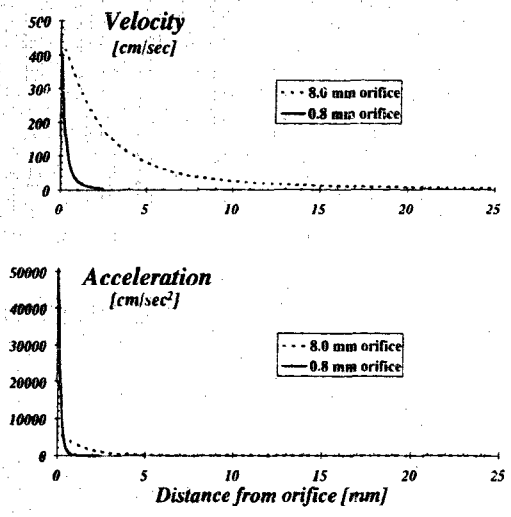

Figure 2. Effect of orifice size on the instantaneous acceleration. Although peak axial centerline velocity is similar for both the 0.8-mm and the 8.0-mm orifice, maximal acceleration is much higher for the smaller orifice, scaling approximately inversely with the orifice diameters.

through a torn bioprosthetic cusp was directed at a sharp angle and collided with the left atrial appendage wall or with the prolapsed cusp. Of the three patients with rapid acceleration, two had a perforation in a degenerated bioprosthetic leaflet and one had multiple small perivalvular leaks around a mechanical prosthesis.

All seven control patients with a free jet had a central jet through a bioprosthesis with a torn cusp, and no other flow disturbance. Of the four patients with slow deceleration, two had a large paravalvular leak and two had a torn cusp with the jets directed in a curved trajectory along an atrial wall.

Numeric simulation. Table 4 summarizes the results of the numeric simulation in each model. In the model of fragmentation the maximal shear stress occurred at the lateral points of

Table 3. Location and Mechanisms of Mitral Regurgitation by Transesophageal Echocardiography

	Patients With Hemolysis (n = 16)	Patients Without Hemolysis (n = 11)
Location		
Central	8 (50%)	9 (82%)
Paravalvular	8 (50%)	2 (18%)
	(p = 0.12, power 0.38)	
Mechanisms		
Fragmentation	2 (12.5%)	0
Rapid acceleration	3 (19%)	0
Collision	11 (69%)	0
Free jet	0	7 (64%)
Slow deceleration	0	4 (36%)
	(p < 0.001, power 0.99)	

Table 4. Results of Numeric Simulation

Mechanism	Maximal Shear Stress (dynes/cm²)
Fragmentation	6,000
Rapid acceleration	4,500
Collision	4,500
Free jet	925
Slow deceleration	950

contact with the solid object, measured in the y axis. The maximal shear value obtained was measured at 6,000 dynes/cm^2. In the collision model the points of maximal shear were located in contact with the vertical wall at the regions where the flow changes direction from the horizontal to the vertical axis. The maximal shear rate obtained was 4,500 dynes/cm^2 measured in the x axis. In both rapid acceleration and free jet models the maximal shear occurred close to the border of the orifice toward the distal flow. The maximal shear rate was 4,500 dynes/cm^2 and 925 dynes/cm^2 in the y axis for each model, respectively. In the slow deceleration model the maximal shear was found at either edge of the orifice and measured 950 dynes/cm^2 in the x axis.

Velocity acceleration. Figure 2 shows the axial components of velocity and acceleration along the centerline leading into 8-mm and 0.8-mm orifices. Although peak velocity is similar in the two cases (given by the Bernoulli equation for a fixed transvalvular gradient), maximal acceleration (both temporal, shown here, and spatial) are much higher for the small orifice, scaling approximately inversely with the orifice diameters.

Discussion

Our study indicates that clinical hemolysis in patients with prosthetic mitral regurgitation is associated with distinct patterns of flow disturbance. These patterns are recognizable by transesophageal echocardiography and are associated with high shear stress by numeric flow simulation. Our findings suggest that hemolysis with prosthetic mitral regurgitation is dependent on the configuration of the flow disturbance in the regurgitant jet and the high shear stress that this produces. An important finding of our study is that the pattern of flow producing hemolysis is independent of the site of origin of the regurgitation and the type of prosthesis implanted. Thus, in our study eight patients (50%) with a central rather than a paravalvular jet had significant hemolysis. Although mechanical valves are most commonly associated with traumatic hemolysis, in our study jets produced by a flail mitral bioprosthesis and by a failed mitral valve repair were also capable of producing a hemodynamic derangement associated with high shear stress and resultant clinical hemolysis.

Etiology of hemolysis. Several mechanisms may contribute to the development of hemolytic anemia with normal and malfunctioning prosthetic valves, including shear stress, turbulence, pressure fluctuations, intrinsic abnormalities of the erythrocyte membrane and interaction with foreign surfaces

(27–29). With the first type of ball-and-cage prostheses implanted, the observed incidence of hemolysis was between 6% and 15% in different series (4,5,12,13). With the improved effective orifice of the tilting disc valves and most bioprostheses, the incidence of hemolysis with normal functioning valves has been significantly reduced (5,14,15). However, hemolysis remains a serious problem in patients with a malfunctioning prosthesis. In early observations, Kastor et al. (4) reported a high association between the incidence of hemolytic anemia and the presence of paravalvular regurgitant leaks. In that series 13% of the valves implanted had a significant paravalvular leak demonstrated by cardiac catheterization, reoperation or autopsy. Of those, 40% had significant hemolysis that required surgical repair or resulted in death. The exact incidence of hemolytic anemia in patients with paravalvular leaks may have been underestimated because many regurgitant leaks were probably undetected before the routine use of echocardiography.

Impact of shear stress. The effects of shear stress causing morphologic alterations in the erythrocyte membrane and resulting in hemolysis have been well studied by Nevaril et al. (21). In their study erythrocyte suspensions were subjected to different shear stress forces in a concentric cylinder viscometer where the conditions of laminar flow were precisely controlled. In blood from normal donors, little hemolysis occurred at stresses <3,000 dynes/cm^2, but at stresses above this level hemolysis greatly increased. The lower limit of shear stress capable of producing detectable hemolysis was ~1,500 dynes/cm^2 in these experiments. These results have been confirmed by other investigators (20,30).

Impact of acceleration. Most prior in vitro work has focused on shear stress as the principal fluid dynamic force responsible for hemolysis. However, our data suggest that acceleration and deceleration may be important causes of hemolysis. Recall that shear reflects the change in velocity as one moves across the flow whereas acceleration and deceleration reflect change in velocity as one moves parallel to the flow.

Collision, with rapid deceleration, was the most common flow pattern associated with hemolysis in our study. For blood moving at velocity v to stop in a distance d requires an acceleration $a = v^2/2d$. To stop a 500-cm/s jet of blood in 0.1 cm thus requires an acceleration of 1,250,000 cm/s^2 or almost 1,300 times the force of gravity *(g)*.

Similarly, we showed that regurgitation through a small orifice is associated with greater hemolysis than is that through large orifices, perhaps owing to the higher acceleration required for passage through the small orifice. For constant orifice velocity, acceleration (dv/dt) scales inversely with orifice size. Higher order derivatives are even more divergent: The "jerk" that a particle is subjected to (d^2v/dt^2) scales inversely with the *square* of orifice size. Acceleration and particle jerk have been little studied in vitro models of hemolysis, but our data suggest that these may be fruitful areas for future investigation.

Other factors. Other factors are also important in the development of hemolytic anemia with prosthetic valves. The interaction of blood with foreign prosthetic material can result in increased hemolysis. This phenomenon was noted with the introduction of the totally cloth-covered ball-and-cage prosthesis (Starr-Edwards, series 2300, 2310) (7,8,31,32). These valves, which were developed in an attempt to decrease the incidence of thromboembolism, were associated with a 15% incidence rate of severe hemolytic anemia. This foreign body effect is of significant importance when considering the probability of developing hemolysis with a malfunctioning prostheses. Teflon and other prosthetic materials that are used to construct the sewing ring and to partially cover the struts in some contemporary valve models become rapidly endothelialized within several weeks after implantation. However, regurgitant jets from paravalvular leaks may denude this endothelium, revealing the prosthetic surface and increasing the propensity to develop hemolysis. This effect of surface interaction appears to be more important at lower shear stress values, as demonstrated by Leverett et al. (18). At shear stress values <1,500 dynes/cm^2, the rate of hemolysis depends more directly on both the area of the contact surface and the time of exposure or shear rate. This area of surface contact is higher and therefore may be an important factor in our model of collision, where peak shear stress values occur at the interface between the regurgitant jet and the wall where it collides. As noted earlier, another important factor that may be implicated in the genesis of hemolysis in this model is the occurrence of deceleration *(g)* forces predisposing to erythrocyte membrane stress. All these reasons may explain why collision was the most frequently observed mechanism in our study patients with hemolysis.

Clinical implications. We have demonstrated that distinct conditions of regurgitant flow—fragmentation, rapid acceleration or collision with a solid wall—are associated with high shear rates and higher rates of hemolysis. Although the indication for valve replacement in the presence of mitral regurgitation may be the hemodynamic significance and the presence of symptoms, the occurrence of hemolysis is independent of the severity of mitral regurgitation. Severe hemolysis resulting in symptomatic anemia can be readily detected clinically; however, some patients may have significant hemolysis that is compensated and not detected clinically but results in long-term complications such as renal hemosiderosis, cardiomyopathy and gallstones. One important observation in the present study is that hemolysis is as likely to occur in the presence as in the absence of central regurgitant orifices. Therefore, the absence of a paravalvular leak does not preclude the development of clinical hemolysis.

Limitations of our study. In our numeric simulation model we incorporated idealized values for orifice sizes and distances to structures. The values used were the averages for the patients with these types of jets in the study group. These conditions may vary from patient to patient and may be difficult to measure exactly with transesophageal echocardiography. However, our purpose was to demonstrate that certain structural characteristics are associated with severe hemolysis in patients with severe mitral

regurgitation. Thus, small single or multiple regurgitant orifices or the presence of flow fragmentation or collision will be more likely to cause hemolysis than will regurgitant jets through larger single orifices with no other apparent flow disturbance.

Our numeric model was constructed in a two-dimensional system. Currently, a three-dimensional model, although possible, requires much computational time, making these calculations very expensive. It also requires accurate three-dimensional structural data, which are only beginning to be available echocardiographically (33). However, to the extent that these flows are axisymmetric, the calculated shear rates should be identical in three-dimensional studies.

We used a fixed viscosity in our numeric model and in calculating shear. Fortunately, the non-Newtonian nature of blood is only apparent at the very lowest shear levels, and thus it is reasonable to assume that this factor did not affect the maximal shear stress calculated in our model.

Finally, we could not account for the effects of variables other than shear, in particular the interaction with a foreign prosthetic surface. The severity of hemolysis may also depend in many cases on the area of exposure and the type of the prosthetic material.

Conclusions. Distinct patterns of regurgitant flow recognizable by transesophageal echocardiography (fragmentation, collision and rapid acceleration) are associated with significant hemolysis in mitral prostheses. In each of these flow patterns numeric simulation demonstrated a high shear rate. Transesophageal echocardiography may be useful in identifying the mechanism of clinical hemolysis in association with prosthetic valve regurgitation.

References

1. DeCesare W, Rath C, Hufnagel C. Hemolytic anemia of mechanical origin with aortic-valve prostheses. N Engl J Med 1965;272:1045–50.
2. Brodeur MT, Sutherland DW, Koler RD, Starr A, Kimsey JA, Griswold HE. Red blood cell survival in patients with aortic valvular disease and ball-valve prosthesis. Circulation 1965;32:570–81.
3. Walsh JR, Starr A, Ritzmann LW. Intravascular hemolysis in patients with prosthetic valves and valvular heart disease. Circulation 1969;39 Suppl I:I-135–40.
4. Kastor JA, Akbarian M, Buckley MJ, et al. Paravalvular leaks and hemolytic anemia following insertion of Starr-Edwards aortic and mitral valves. J Thorac Cardiovasc Surg 1968;56:279–88.
5. Rodgers BM, Sabiston DC. Hemolytic anemia following prosthetic valve replacement. Circulation 1969;39 Suppl I:I-155–61.
6. Eyster E, Rothchild J, Mychajliw O. Chronic intravascular hemolysis after aortic valve replacement. Long term study comparing different types of ball-valve prostheses. Circulation 1971;44:657–65.
7. Boruchow IB, Ramsey HW, Wheat MW. Complications following destruction of the cloth covering of a Starr-Edwards aortic valve prosthesis. J Thorac Cardiovasc Surg 1971;62:290–3.
8. Santinga JT, Kirsh MM. Hemolytic anemia in series 2300 and 2310 Starr-Edwards prosthetic valves. Ann Thorac Surg 1972;14:539–44.
9. Harken DE, Soroff HS, Taylor WJ, Lefemine AA, Gupta SK, Lunzer S. Partial and complete prostheses in aortic insufficiency. J Thorac Cardiovasc Surg 1960;40:744–62.
10. Harken DE, Taylor WJ, LeFemine AA, et al. Aortic valve replacement with a caged ball valve. Am J Cardiol 1962;9:292–9.
11. Starr A, Edwards ML. Mitral replacement: clinical experience with a ball-valve prosthesis. Ann Surg 1961;154:726–40.
12. Pirofsky B. Hemolysis in valvular heart disease. Ann Intern Med 1966;65: 373–6.
13. Clark RE, Grubbs FL, McKnight RC, Ferguson TB, Roper CL, Weldon CS. Late clinical problems with Beall model 103 and 104 mitral valve prostheses: hemolysis and valve wear. Ann Thorac Surg 1976;21:475–82.
14. Emery RW, Anderson RW, Lindsay WG, Jorgensen CR, Wang Y, Nicoloff DM. Clinical and hemodynamic results with the St. Jude medical aortic valve prosthesis. Surg Forum 1979;30:235–8.
15. Rao KM, Learoyd PA, Rao RS, Rajah SM, Watson DA. Chronic haemolysis after Lillehei-Kaster valve replacement. Comparison with the findings after Bjork-Shiley and Starr-Edwards mitral valve replacement. Thorax 1980;35: 290–3.
16. Marbager JP, Clark RE. The clinical life history of explanted prosthetic heart valves. Ann Thorac Surg 1982;34:22–33.
17. Rutledge R, Applebaum RE, Kim JB, Engler MB, Engler MM. Actuarial analysis of the risk of undergoing repeat cardiac valve surgery. Am J Surg 1984;148:357–61.
18. Leverett LB, Hellums JD, Lynch EC. Red blood cell damage by shear stress. Biophys J 1972;12:257–73.
19. MacCallum RN, Lynch EC, Hellums JD, Alfrey CP. Fragility of abnormal erythrocytes evaluated by response to shear stress. J Lab Clin Med 1975;85: 67–74.
20. Shapiro SI, Williams MC. Hemolysis in simple shear flows. AICHE (Am Inst Chem Eng) Symp Ser 1970;16:575–80.
21. Nevaril CG, Lynch EC, Alfrey CP, Hellums JD. Erythrocyte damage and destruction induced by shearing stress. J Lab Clin Med 1968;74:784–90.
22. Mugge A, Daniel WG, Frank G, Lichtlen PR. Echocardiography in infective endocarditis: reassessment of prognostic implications of vegetation size determined by the transthoracic and the transesophageal approach. J Am Coll Cardiol 1989;14:631–8.
23. Daniel WG, Mugge A, Martin RP, et al. Improvement in the diagnosis of abscesses associated with endocarditis by transesophageal echocardiography. N Engl J Med 1991;324:795–800.
24. Nellesen U, Schnittger I, Appleton CP, et al. Transesophageal two-dimensional echocardiography and color Doppler flow velocity mapping in the evaluation of cardiac valve prostheses. Circulation 1988;78:848–55.
25. Castello R, Lenzen P, Aguirre F, Labovitz AJ. Quantification of mitral regurgitation with Doppler color flow mapping: correlation with cardiac catheterization. J Am Coll Cardiol 1992;19:1516–21.
26. Castello R, Pearson AC, Lenzen P, Labovitz AJ. Effect of mitral regurgitation on pulmonary venous velocities derived from transesophageal echocardiography color-guided pulsed Doppler imaging. J Am Coll Cardiol 1991; 17:1499–506.
27. Rand RP, Burton AC. Mechanical properties of the red cell membrane. I. Membrane stiffness and intracellular pressure. Biophys J 1964;4:115–35.
28. Rand RP. Mechanical properties of the red cell membrane. II. Viscoelastic breakdown of the membrane. Biophys J 1964;4:303–16.
29. Weed RI, Reed CF. Membrane alterations leading to red cell destruction. Am J Med 1966;41:681–98.
30. Williams AR, Hughes DE, Nyborg WL. Hemolysis near a transversely oscillating wire. Science 1970;169:871–3.
31. Schottenfeld M, Wisheart JD, Ross JK, Lincoln JC, Ross DN. Cloth destruction and haemolysis with totally cloth-covered Starr-Edwards prostheses. Thorax 1971;26:159–62.
32. Santinga JT, Batsakis JT, Flora JD, Kirsh MM. Hemolysis in the aortic prosthetic valve. Chest 1976;69:56–61.
33. Pandian NG, Hsu TL, Roelandt J, et al. Dynamic three-dimensional echocardiography: methods and clinical potential. Echocardiography 1994, 11:237–59.